WPCA NEWS
Worldwide Pollution Control Association
www.wpca.info

A Bi-Annual Newsletter Sponsored by the WPCA Summer - 2015

Executive Summary

Beneficial Consequences of SCR Catalyst Replacement at New Harquahala Units 1 and 2

By Jessica Muncy and Tom Martz, FERCo; Wayne Jones, Haldor Topsoe; Chris Bates, New Harquahala Gen. Co.

A discussion of some beneficial economic and operating consequences gained by replacing the SCR catalyst on two of the three units at the Harquahala Generating Company combined cycle natural gas plant in Tonopah, AZ. Specifically this article provides a detailed analysis of benefits resulting from reduced pressure drop and decreased and steadier ammonia injection across the two SCRs with new catalyst as compared to the identical control unit.

Full Story….

Taking the Mystery out of Choosing Electrostatic Precipitator (ESP) Power Supplies for MATS PM Control

By David F. Johnston, John A. Knapik, B&W and John Walker, formerly with Duke Energy, Wabash River Station, W. Terre Haute, Indiana

A good modelling and laboratory comparison of the pros and cons of the available ESP power supplies including the traditional single phase 60 hertz TRs, high frequency Switch Mode Power Supplies and the new three phase 60 hertz design already popular in Europe. This article includes test results of the new 3 phase 60 hertz TR verses the traditional single phase TR at an American plant which demonstrated a 50% improvement in average power.

Full Story….

Acid Gas Control Technologies / Challenges of Retrofitting Dry / Semi-Dry Scrubbing Technologies

By Kevin Cosman, KC Cottrell Inc.

With a variety of technologies currently available to retrofit dry or semi dry scrubbing technologies, end users must be more vigilant in understanding the pros and cons of each. This article discusses specific considerations when simultaneously trying to reuse existing equipment and retrofitting new technologies

Full Story….

The Use of Flue Gas Mixing Technology for Improving In-Duct Sorbent Injection System Performance

By Matthew Quitadama, Babcock Power Environmental Inc.

The effectiveness of dry sorbent injection systems depends on several factors such as sorbent properties, choice of injection location, type of particulate control device, and injection system design. For the last of these factors, injection system design, there has become a major focus on improving sorbent mixing/dispersion via static mixers to provide consistent sorbent coverage across the full range of operating conditions.

Full Story….

WPCA NEWS
www.wpca.info
A Bi-Annual Newsletter Sponsored by the WPCA
Summer 2015

WORLDWIDE POLLUTION CONTROL ASSOCIATION

Beneficial Consequences of SCR Catalyst Replacement at New Harquahala Units 1 and 2

By Jessica Muncy & Tom Martz, FERCo; Wayne Jones, Haldor Topsoe; Chris Bates, New Harquahala Gen. Co.

ABSTRACT

The New Harquahala Generating Co. (NHGC) combined-cycle plant consists of three identical 1 x 1 units for a total of 1,092 MW. The units are equipped with SCR (Selective Catalytic Reduction) for NOx emissions control. In 2011, plant operators were finding it increasingly difficult to comply with the stack NOx permit limits during startup, particularly on Units 1 and 2. Laboratory analyses of SCR catalyst samples indicated significant catalyst deactivation. In order to avoid possible NOx permit violations, the original Unit 1 and Unit 2 catalyst charges were replaced with Haldor Topsoe corrugated catalyst in April 2012. To quantify the impacts of the catalyst replacement, pre and post replacement operating data were analyzed. There were several beneficial consequences of the catalyst replacement, including a decrease in pressure drop (i.e., improved engine efficiency), a decrease in normalized ammonia consumption and improved SCR performance during start up.

INTRODUCTION

The New Harquahala Generating Co. (NHGC) combined-cycle plant is located in Tonopah, Arizona, approximately 60 miles west of Phoenix. The 1,092 MW plant consists of three identical 1 x 1 units utilizing Siemens SGT6-6000G gas combustion turbines. The units are equipped with SCR (Selective Catalytic Reduction) for NOx emissions control. Hitachi Zosen provided the original corrugated style SCR catalyst charges in 2003 when the units were commissioned.

In 2011, plant operators were finding it increasingly difficult to comply with the stack NOx permit limits during start up. Units 1 and 2 were particularly problematic. At that time, although the chronological age of the units was 8 years, the actual logged run time was on average only 2200 hours for each unit. Laboratory analyses of SCR catalyst samples performed in 2011 indicated significant catalyst deactivation. To avoid possible permit violations, the original SCR catalyst charges in Units 1 and 2 were replaced with Haldor Topsoe corrugated catalyst in April 2012.

Since replacing the SCR catalyst, NHGC operators have reported improved SCR performance on Units 1 and 2, especially during start up. In order to quantify the beneficial consequences of the catalyst replacement from an overall plant performance view, pre and post replacement operating data were analyzed.

The analysis included data from Units 1, 2, and 3. The Unit 3 data served as a convenient control since the Unit 3 catalyst was not replaced. The data sets included gas turbine operation parameters such as load, fuel flow, ammonia flow, temperatures, catalyst pressure drop and NOx and O_2 emissions. The relevant data sets were isolated and plotted to assist with visualizing the performance improvements. These plots included:

- Catalyst pressure drop
- Ammonia flow
- Inlet NOx
- Ammonia consumption ratio (pounds ammonia per pound of NOx removed)
- Startup ammonia flow

In addition, calculations were performed to estimate fuel and ammonia cost savings generated by the catalyst replacement.

DATA SET DESCRIPTION

Eight (8) data sets from each unit were included in the study. The data sets included periods before and after

the April 2012 catalyst replacement on Units 1 and 2, and represented either start-up or normal operation. Start-up data sets consisted of nominally 17 hours of data, typically starting at midnight, and included time periods when the unit was coming on line. Normal operating data consisted of 48 hours of data, starting and ending on midnight of two consecutive days.

Although the Unit 3 catalyst was not replaced, Unit 3 data were included in the analysis as a control. Furthermore, the catalyst pressure drop transmitters on all of the units were not operating properly prior to April 2012, at which point they were repaired. As a result, the post April 2012 Unit 3 pressure drop data (i.e., still with the original catalyst) were used to represent Units 1 and 2 before the catalyst change.

In general, more data were provided for the pre change period than post change. This was due to the relatively low capacity factor for these units, and the fact that the catalyst charges were replaced only one year ago.

SCR CATALYST PRESSURE DROP

Since SCR catalyst pressure drop impacts engine efficiency, an important objective of the data analysis was to quantify differences in this parameter before and after the SCR catalyst change.

Figure 1 shows a comparison of pressure drop through the new Haldor Topsoe catalyst on Units 1 and 2 to the original Hitachi Zosen catalyst on Unit 3. Pressure drop is shown as a function of the calculated flue gas flow rate (F-factor method) using fuel flow, stack O_2, and an assumed average heating value of 21,000 Btu/lb for natural gas. Start-up data were not included in Figure 1, as catalyst pressure drop was load dependent and the pressure drop reduction was quantified for higher, more consistent, load ranges.

The data in Figure 1 show that the catalyst pressure drop decreased significantly after the catalyst replacement in April 2012. The average pressure drop measured for the load range of 185 MW - 195 MW on Unit 3 was 2.9” wc (original Hitachi Zosen catalyst), while the Unit 1 average was 1.1” wc and the Unit 2 average was 1.3” wc (new Haldor Topsoe catalyst).

ENGINE PERFORMANCE CURVES

Improvements in engine efficiency due to the reduced system back pressure (i.e., lower catalyst pressure drop) were small on a percentage basis (fractions of a percent), making it impractical to extract meaningful fuel savings results

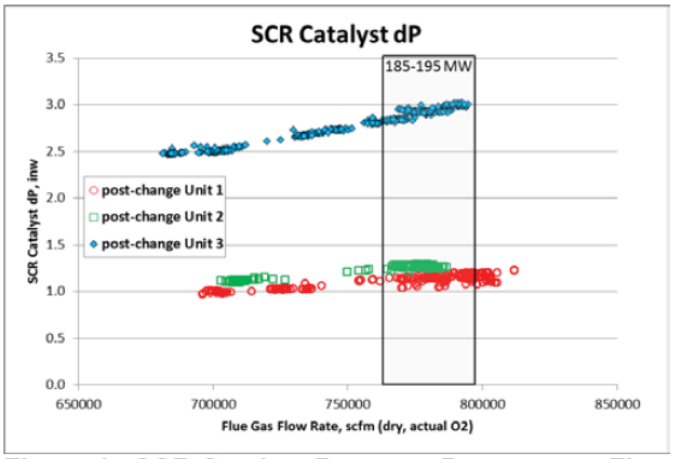

Figure 1. SCR Catalyst Pressure Drop versus Flue Gas Flow Rate (startup data removed)

from small pockets of operating data. Therefore, in order to better quantify fuel savings and increases in gross power output, the engine performance correction curves for the SGT6-6000G engines from Siemens were used. The curves for the SGT6-5000F engines, which are similar in performance to the 6000G engines, are referenced in Figure 2. These performance correction curves provided linear relationships between gross power and heat rate as a function of pressure loss.

Table 1 presents the estimated heat rate and fuel savings for Units 1 and 2. The average catalyst pressure drop data from 185 MW -195 MW on Unit 1 decreased by 1.8” wc, and decreased by 1.6” wc on Unit 2. Per the performance correction curve, this resulted in a gross heat rate correction factor of 0.9984 and 0.9985 for Units 1 and 2, respectively. If the average heat rate is assumed to be 10,000 Btu/KWh and the heating value for natural gas is assumed to be 21,000 Btu/lb, this resulted in a calculated fuel savings of only 0.16% for Unit 1 and 0.15% for Unit 2. While this fuel savings does add up on an annual basis, it is not within the measurable ranges of the instrumentation, which measure on a KPPH basis. For instance, for Unit 1, the change in fuel flow would be only approximately 0.15 KPPH, which is not within the detection limits. However, if natural gas prices are assumed to be $3.50/MBtu, the annual fuel savings (based on 8000 operating hours) are estimated to be $80,000 - $90,000 for each unit.

Table 2 presents the estimated increase in gross power output based on the reduced pressure drop. Using the engine performance curves, a gross power correction factor of 1.003 was calculated for Unit 1 and 1.002 for Unit 2; or ap

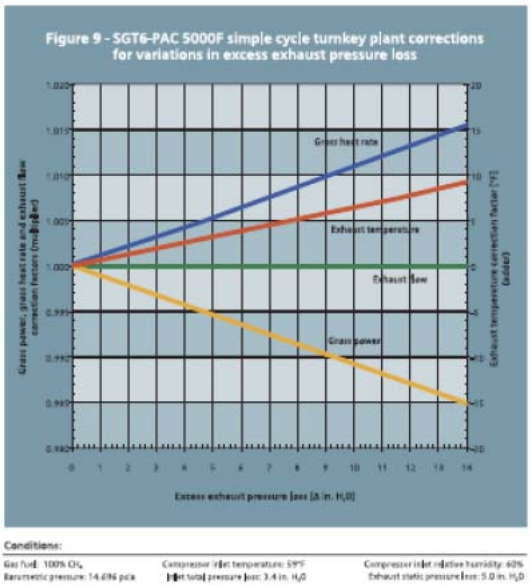

Figure 2. SGT6-PAC 5000F Siemens Engine Performance Correction Curves

Table 1. NHGC Units 1 and 2 Estimated Heat Rate and Fuel Savings

	Avg dP deviation 185-195 MW	Gross Heat Rate Correction	Fuel Savings, %	Fuel Savings, $/annually (8000 hrs)
Unit 1	-1.8 " wc	0.9984	0.16	$87,000
Unit 2	-1.6" wc	0.9985	0.15	$81,200

Table 2. NHGC Units 1 and 2 Estimated Increase in Gross Power Output

	Avg dP deviation 185-195 MW	Gross Power Correction	Power Increase (190 MW Base)	Profit, $/annually (8000 hrs)
Unit 1	-1.8" wc	1.003	0.49 MW	$39,000
Unit 2	-1.6" wc	1.002	0.45 MW	$36,000

proximately 0.5 MW for each unit. Assuming the plant sold the additional power at a gross margin of $10/MWh, this represented a $35,000 - $40,000 gain in annual revenue from each unit for 8000 hours of increased load operation.

SCR AMMONIA CONSUMPTION

Another important objective of the data analysis was to quantify differences in ammonia consumption before and after the SCR catalyst change. Since the original catalyst had deactivated significantly, the catalyst replacement was expected to reduce the amount of wasted ammonia (i.e., ammonia slip) at higher NOx removal efficiencies.

Ammonia flow data for NHGC Unit 1 before and after catalyst replacement are shown in Figure 3. The data are shown as a function of load, and do not include start-up periods. The plot illustrates that the upward scatter in the ammonia flow and average flow at a given load was generally much greater before the catalyst change than after. Since ammonia flow is tied directly to the SCR catalyst inlet NOx level, it was suspected that variations in the engine outlet NOx level were responsible for some portion of the scatter in ammonia flow.

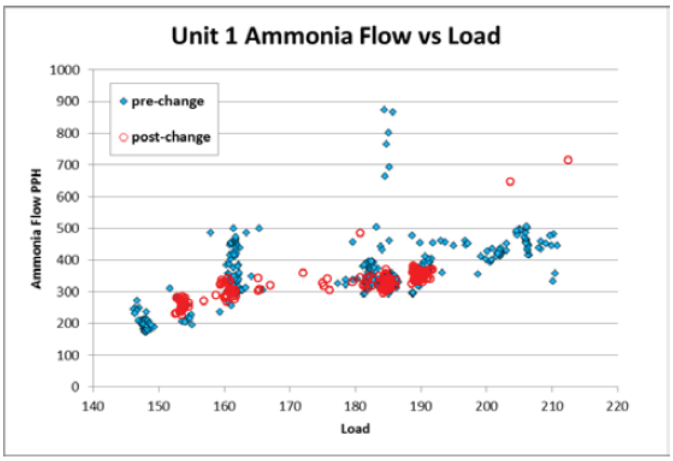

Figure 3. NHGC Unit 1 Ammonia Flow versus Load (4/15/2010 and startup data removed)

This suspicion was confirmed when ammonia flow was plotted against the catalyst inlet NOx measurements. Figure 4 (page 4) shows the inlet NOx variation for Unit 1 was much greater prior to the catalyst replacement (5 ppm to 40 ppm) than after (20 ppm - 30 ppm). The change in engine NOx variation was not directly caused by the SCR catalyst replacement, but rather a change in engine operation that apparently coincided with the catalyst replacement.

In order to accurately isolate the change in ammonia consumption due only to the catalyst replacement, it was necessary to eliminate inlet NOx as a variable. To do this, the ratio of pounds of ammonia injected per pound of NOx removal (i.e., the ammonia consumption ratio) was plotted against load, as shown in Figure 5 (pg. 4). The upward scatter in this ratio prior to the catalyst change represented wasted ammonia flow in the form of ammonia slip. Since the original catalyst had deactivated significantly, the operators were forced

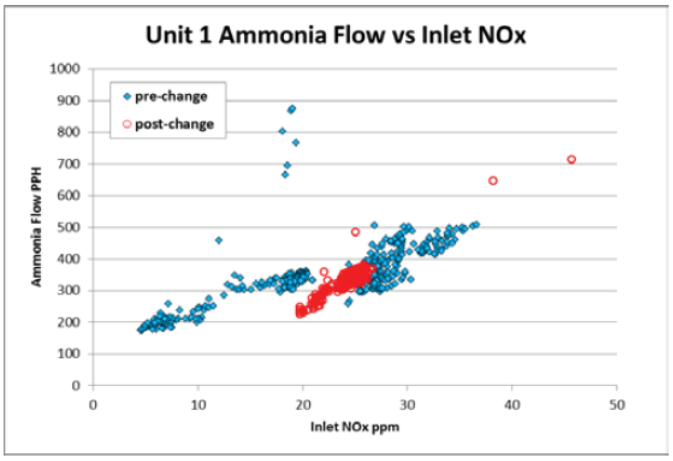

Figure 4. NHGC Unit 1 Ammonia Flow versus Inlet NOx (4/15/2010 and startup data removed)

to over-inject ammonia to meet the required stack NOx levels. The amount of wasted ammonia was clearly reduced when the new catalyst was installed.

Data for Unit 2 displayed similar trends and degrees of scatter as the Unit 1 data. The ammonia consumption ratios for Units 1 and 2 are summarized in Table 3 for data before ("pre") and after ("post") the catalyst replacement. Comparison of the ammonia consumption ratio for Unit 1 shows that it decreased by 36% overall, and by 23% for a narrower load range of 180MW -190MW. The ammonia consumption ratio for Unit 2 decreased less, with 13% overall and 10% for the 180MW -190MW load range.

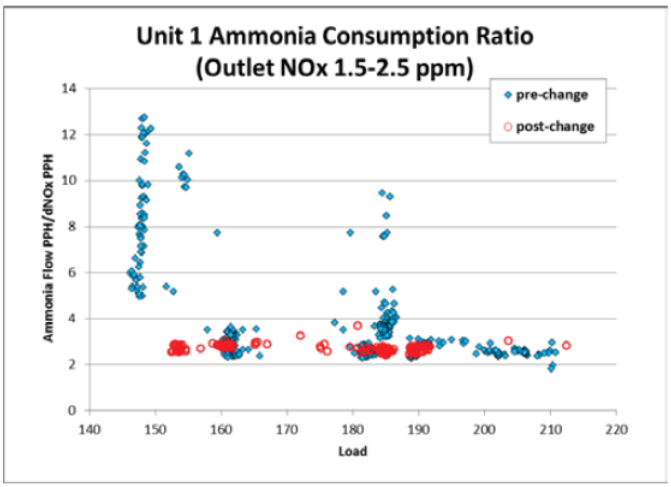

Figure 5. NHGC Unit 1 Ammonia Consumption Ratio versus Load (4/15/2010 and startup data removed)

The Unit 3 data served as a control for the ammonia consumption analysis, since the units are identical and the SCR catalyst was not replaced on Unit 3. The ammonia flow for Unit 3 is shown as a function of load and SCR inlet NOx in Figures 6 and 7, and the ammonia consumption ratio is shown in Figure 8. Data are included before and after the April 2012 catalyst replacements on Units 1 and 2. It is important to note that the scatter in the SCR inlet NOx did not significantly change between these time periods, indicating that changes in engine operation were not implemented on Unit 3 as they were on Units 1 and 2.

Furthermore, the Unit 3 ammonia consumption ratio data were consistent in the overall ammonia consumption and in the degree of variation. The average overall ammonia consumption ratio prior to 2012 was 3.1 and the overall average after 2012 was 3.2. Since the Unit 3 catalyst was not replaced and the data trends remained essentially unchanged, these figures demonstrate that the ratio differences shown for Units 1 and 2 do correlate to the catalyst replacement.

Table 3. NHGC Unit 1 and 2 Percent Decrease in Ammonia Consumption Ratio

	Unit 1		Unit 2	
	Pre-	Post-	Pre-	Post-
140-220 MW	4.2	2.7	3.1	2.7
	36%		13%	
180-190 MW	3.4	2.6	2.9	2.6
	23%		10%	

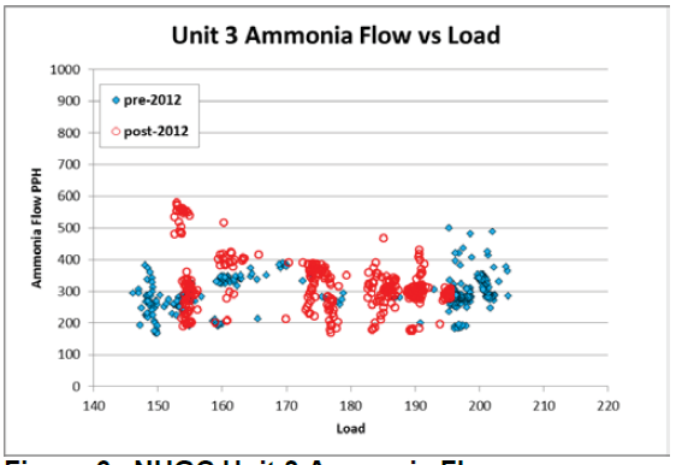

Figure 6. NHGC Unit 3 Ammonia Flow versus Load (startup data removed)

POTENTIAL AMMONIA COST SAVINGS

The potential ammonia costs savings for NHGC Units 1 and 2 were calculated using a 19% aqueous ammonia price of $1000/ton and are summarized in Table 5. The cost savings were first calculated for a wide load range (140MW -220MW), and then for a narrow load range closer to full

load (180MW -190MW). The calculations assumed a constant NOx reduction of 20 ppm for both units before and after the catalyst replacement, and factored in the actual ammonia consumption ratios listed in Table 3.

The hypothetical costs are presented on an annual (8000 hr) basis. As seen in Table 5, the potential savings varied widely, depending on the unit and the load range. Across the wider load range, the savings were estimated to range from $170,000 to $650,000 annually. However, the saving were less between 180MW -190MW, ranging from $120,000 to $350,000 annually. This reflected the inconsistent pattern of ammonia over-injection prior to the catalyst replacement.

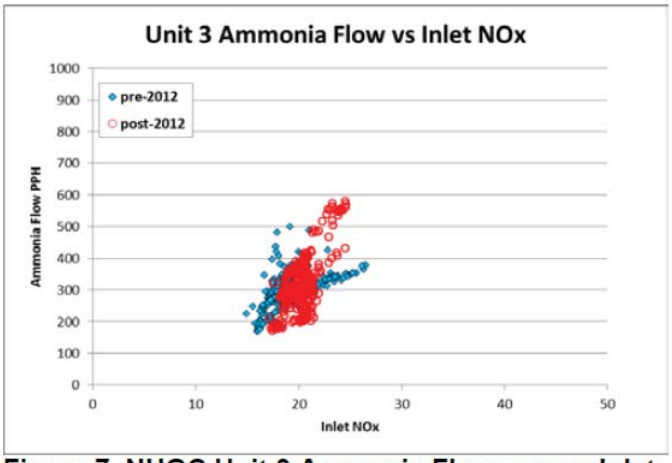

Figure 7. NHGC Unit 3 Ammonia Flow versus Inlet NOx (startup data removed)

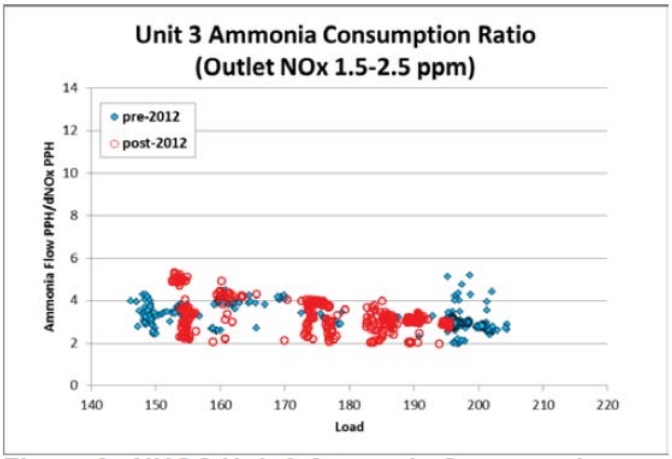

Figure 8. NHGC Unit 3 Ammonia Consumption Ratio versus Load (startup data removed)

SCR STARTUP PERFORMANCE

It was noted previously that data from Units 1 and 2 prior to the catalyst replacement had significant upward variations in the ammonia consumption ratio compared to the post-replacement data. These variations were indicative of the need to over-inject ammonia since the catalyst had significantly deactivated. Similar trends were seen in the startup data for Units 1 and 2.

Table 4. NHGC Units 1 and 2 Potential Ammonia Consumption Cost Savings

	Savings $/yr 140-220MW	Savings $/yr 180-190MW
Unit 1	$650,000	$350,000
Unit 2	$170,000	$124,000

Figure 9 shows the Unit 2 ammonia consumption ratio for four (4) separate startup periods as a function of time. Three periods were provided prior to the catalyst replacement, and one afterward. The data illustrate how operators had to inject excess ammonia prior to the catalyst change in order to achieve the stack NOx set point. In contrast, the ammonia consumption ratio was lower and steadier during the post-change start up in June 2012. The Unit 1 startup data presented a similar improvement. However, the Unit 1 ammonia flow transmitter was not operational during the first seven hours of start up for the data set following the catalyst replacement (zero flow during this time).

For comparison, Figure 10 (page 6) shows the Unit 3 ammonia consumption ratio for three startup periods prior to April 2012, and one afterward. The plot shows that the post-change ammonia consumption ratio trends are similar to the pre-change data, further demonstrating that the ammonia consumption differences shown for Units 1 and 2 can be correlated to the catalyst replacement.

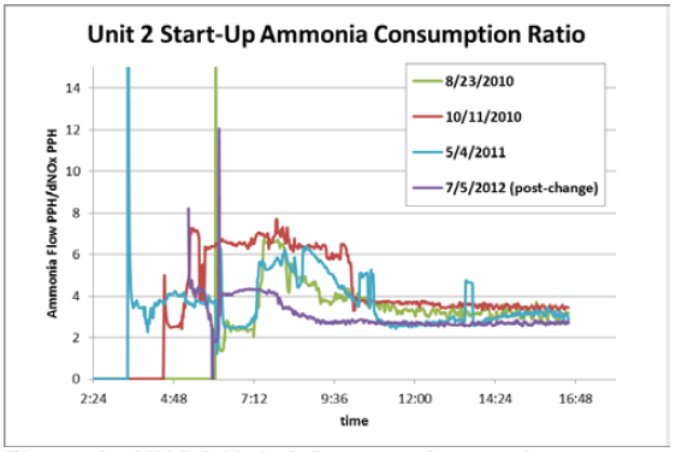

Figure 9. NHGC Unit 2 Start-up Ammonia Consumption Ratio versus Time

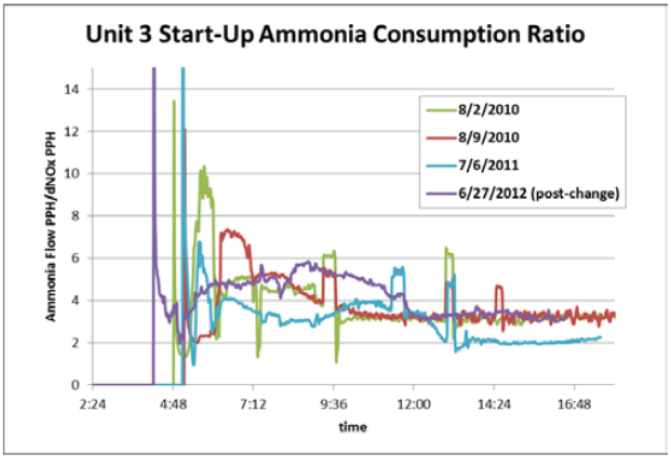

Figure 10. NHGC Unit 3 Start-up Ammonia Consumption Ratio versus Time

CONCLUSIONS

The original Unit 1 and Unit 2 SCR catalyst charges were replaced with Haldor Topsoe corrugated catalyst in April 2012. There were several beneficial consequences of this action from an overall plant performance view, as described below.

- The catalyst pressure drop was reduced by nominally 1.7" wc on each unit, resulting in fuel savings of 0.16% based on the engine back pressure correction curves. Assuming 8,000 hours of annual operation, this represented a cost reduction of approximately $80,000 – $90,000 per unit.

- The reduction in pressure drop also provided nominally 0.5 MW of additional gross power output for each unit. Assuming the plant sold the additional power at a gross margin of $10/MWh, this represented a $35,000 - $40,000 gain in annual revenue from each unit for 8000 hours of increased load operation.

- Prior to the catalyst replacement in April 2012, operators were forced to over-inject ammonia to meet the required stack NOx levels. This was because the original catalyst had significantly deactivated. After the new catalyst was installed, the amount of wasted ammonia (i.e., ammonia slip) was clearly reduced. The potential savings varied, depending on the unit and the load range. The ammonia consumption across a load range of 140MW to 220MW (corrected for inlet NOx variations) was reduced by as much as 36% for Unit 1 and 14% for Unit 2. This represented a potential cost savings range of $170,000 to $650,000 on an annual (8000 hr) basis. However, the potential savings were less between 180MW -190MW, ranging from $120,000 to $350,000 annually. This reflected the inconsistent pattern of ammonia over-injection prior to the catalyst replacement.

- Startup data prior to the catalyst replacement also indicated that operators were forced to over-inject ammonia to meet the required stack NOx levels. After the catalyst change, the ammonia consumption ratio was lower and steadier during start up, and operators no longer reported issues with respect to NOx compliance.

For further information contact Wayne Jones at wsj@topsoe.com

HALDOR TOPSØE

Taking the Mystery out of Choosing Electrostatic Precipitator (ESP) Power Supplies for MATS PM Control

By David F. Johnston, John A. Knapik, Babcock & Wilcox, and
John Walker, formerly with Duke Energy, Wabash River Station, W. Terre Haute, Indiana

ABSTRACT

Many coal-fired power plants will upgrade their aging electrostatic precipitators (ESPs) to meet the particulate matter (PM) emissions requirements established by the Mercury and Air Toxics Standards (MATS) established by the U.S. Environmental Protection Agency (EPA). Many of those upgrades will likely entail the replacement of existing conventional power supplies [transformer rectifier (TR) sets].

While the conventional single-phase power supplies have been the norm for more than 60 years, in large part due to a stellar reliability record, new types have been introduced into the marketplace. The high frequency switch mode power supply (SMPS) was launched in the 1990s. During its early stages, the SMPS was plagued with a high rate of failure which has improved, but has not achieved the reliability of single-phase. An even newer introduction, especially popular in Europe, is the 3-phase rectified power supply, which inherited many of the reliability benefits of its single-phase predecessor. Not much has been reported on the development and performance of the 3-phase low frequency power supply.

In this article, the results of ESP power supply modeling and laboratory testing will be presented for multiple types of precipitator power supplies. In addition, the results of field testing of a single-phase and a low frequency 3-phase power supply are presented. This article highlights the key features, advantages, and disadvantages of each device, with the intent to help the end user in the technology selection process. Several factors that affect this decision will be discussed, including the amount of ripple in the secondary voltage waveform, increased power in the precipitator field, harmonic distortion, equipment size, weight and footprint, cost, and reliability.

The results imply that low ripple power supplies hold a distinct advantage over the conventional single-phase power supply because of their ability to apply more power to the precipitator field. The results further indicate that the 3-phase power supply (a low frequency design) has an advantage over other types of low ripple power supplies because of its higher reliability and lower cost, albeit in a larger, heavier package.

INTRODUCTION

To meet particulate matter (PM) requirements of the Mercury and Air Toxics Standards (MATS), stack emissions of filterable particulate must be controlled below a level of 0.03 lb/mm Btu. This new requirement is likely to demand improved performance from existing ESPs. In addition, there are tougher demands on maintainability of this lower emissions requirement. Not only are the emissions to be reduced, they must remain low for longer periods of time.

One of the fundamental means to improve the performance of an existing ESP is to boost its corona power. The relationship between specific corona power (watts/1000 acfm) and collection efficiency has been well researched[1-3]. So, while optimization efforts to increase efficiency (e.g., a simple re-build of the ESP or adding additional plate area through increased height or additional fields) almost always entail a replacement of the existing power supplies, additional questions arise: what type of power supply can boost the corona power output, and how to manage the new challenges of higher availability when switching power supplies. A study was conducted to evaluate the key features, advantages and disadvantages, of each type of power supply.

BRIEF HISTORY OF ESP POWER SUPPLIES

ESP power supplies have come a long way from the early days of a separate high voltage transformer and a mechanical rectifier which energized the high voltage electrodes in the ESP. The mechanical rectifier used a four-pole synchronous motor driving four pairs of discharge brushes. The synchronous contact of the brushes provided a pulsating unidirectional current.

Those early power supplies did not have an automatic voltage control, which was first patented in 1952.[4] To control ESP voltage, a manually operated switchboard was utilized with multiple taps on the primary side of the high voltage transformer. In the 1950s, mechanical rectifiers were replaced by selenium rectifiers, integral with the transformer. In the mid-1960s, silicon diodes replaced the selenium rectifiers. These diodes were more compact, had a lower forward resistance, and did not age.[5]

Analog automatic voltage controls and silicon controlled rectifiers (SCRs) were the standard for many years. The advent of microprocessors resulted in patented control algorithms,[6-8] more precise control of the power applied to the precipitator, and software integration with other plant systems.

All of these advances were limited since the single-phase precipitator power supply has a voltage waveform with a significant amount of ripple as shown in Figure 11.

The ripple reduces how much power can be applied to the

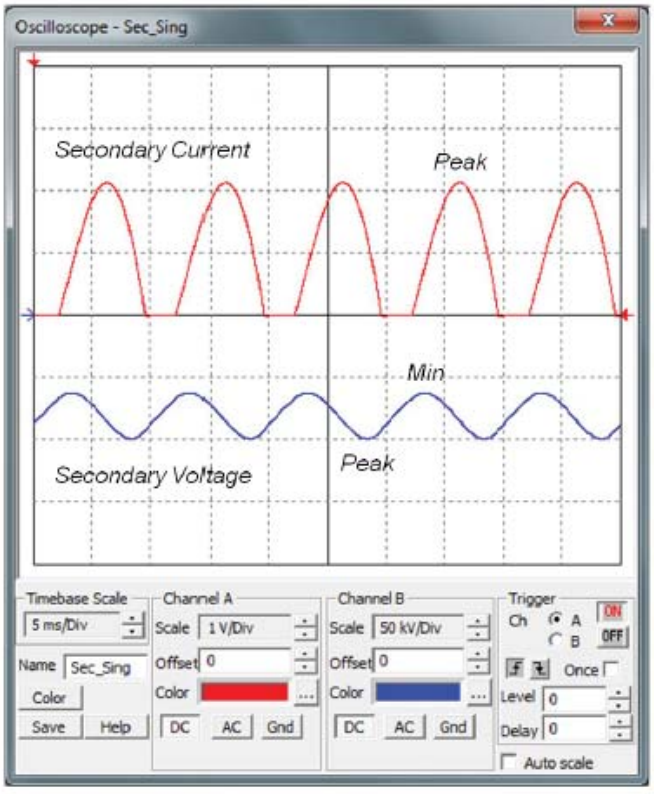

Figure 11: Single-Phase Precipitator Power Supply Voltage and Current

precipitator field. There is a practical limit to how much voltage can be applied to a precipitator field due to sparking, and sparking occurs at the peak of the secondary voltage waveform. The resultant average voltage is always lower than the peak voltage by about 20%. Manufacturers recognized if this waveform could be changed by making the average voltage equal to the peak voltage, significantly more power could be applied to the precipitator field. Many novel approaches have been tried to accomplish this, including placing a filter on the output of the single-phase precipitator power supply to remove the ripple.[9,10]

Today, in addition to the single-phase precipitator power supply with its rippled voltage waveform, a variety of low ripple power supply options is available. Each of these removes the ripple from the secondary voltage waveform and provides a low peak-to-average-voltage ratio. The earliest among these was the high frequency switch mode. It was designed to provide increased power to the precipitator field while having less size and weight, symmetrical 3-phase load, and higher power factor, all with high reliability.

In actual practice, however, the reliability has been less than anticipated (with a record that is much less impressive than the single-phase precipitator power supply). In addition, there have been grounding and shielding issues coupled with high input and output harmonic distortion.

Based on these experiences, and the many choices available in precipitator power supplies, B&W conducted an internal study utilizing power supply electrical models, laboratory and field testing to compare different power supply types. Since it had been reported that the Europeans were successfully utilizing low frequency 3-phase precipitator power supplies to achieve a low ripple voltage waveform, this type of power supply was also evaluated. The outcome of the study indicated potential benefits of the low frequency 3-phase precipitator power supply, which led to the development of a low frequency 3-phase precipitator power supply and field testing for further verification.

MODELING PRECIPITATOR POWER SUPPLIES

Accurately comparing precipitator power supplies presents unique challenges. Precipitator power supplies cannot be installed on the exact same precipitator field at the exact same time and experience the exact same conditions. In addition, in an operating plant, it is unreasonable to expect that the precipitator power supply will experience every possible upset condition. This results in equipment that does not get fully tested and requires product enhancement and develop-

ment to be conducted in the field, often at great inconvenience and expense to the plant owner. Thus, we decided to begin our research process by using electrical modeling of typical power supplies used on ESPs.

For this project, an independent electrical model was created for each type of precipitator power supply. Once an accurate software model was created, each precipitator power supply was operated under a large number of operating conditions and the results evaluated. In addition to electrical performance, modeling software is useful for analyzing other areas including component heating (which is helpful in predicting reliability).

The greatest efficiency and best operation will be achieved if the precipitator power supply is properly matched to the precipitator load. For example, it is better to size a power supply to operate at 70 to 100% of its rating rather than 10 to 30% of its rating. It is therefore important to understand the electrical nature of the precipitator load. In its most simplified version, the precipitator load can be shown as a capacitor in parallel with a resistor.

The precipitator field has a capacitive characteristic. The basic construction of a capacitor is two conductors separated by a dielectric or insulator. The ESP collecting plates form one conductor, while the discharge electrodes form the other; the gas path between them forms the dielectric. Because the properties of the dielectric are affected by the gas that is being treated, a unique capacitor is created. A reasonable estimate (which has been used by us and by others) of the value of this capacitor for a properly matched and sized power supply is approximately 10 nf per milliamp of power supply. For a 1000 milliamp power supply this would be approximately 0.1 µf.

There are several fundamental properties of capacitors that are important to our understanding of the precipitator power supply. Ideal capacitors do not dissipate energy but store it in the form of an electric field. Therefore, even if the power supply would have a high ripple output, once the power supply is connected to the precipitator, its capacitive characteristic filters or reduces the ripple in the output voltage waveform. This is very important and explains why very low ripple in the output voltage waveform can be achieved even with low frequency power supplies.

The load resistor on the power supply dissipates energy. A reasonable estimate (which has been used by us and by others) of the value of this resistor for a properly matched and sized power supply can be found by dividing the average voltage rating of the power supply by the average milliamp rating. For example, a precipitator power supply rated at 80 kV and 1000 milliamps would yield a value of 80 KΩ for the load resistor. This indicates that for maximum power transfer, the precipitator power supply in this example should be matched to an 80 KΩ load.

In actual practice, the precipitator load of our example would rarely be exactly 80 KΩ and can vary over a significant range. If the precipitator power supply is not experiencing sparking and the actual load is less than 80 KΩ, then the precipitator power supply will operate at a current limit. If the precipitator power supply is not experiencing sparking and the actual load is more than 80 KΩ, then the precipitator power supply will operate at a voltage limit. The precipitator power supply should therefore accommodate a broad load range. Unfortunately, some high frequency designs have a turn-down limitation (typically 10%). This means the power supply cannot operate below this turn-down rating. This has been a problem in some applications that have a significant load swing or during start-up of the ESP.

The results of the model study are shown in Table 5 (page 10); these results will be examined in detail later in this paper. The data indicated very good performance of the low frequency 3-phase precipitator power supply to produce a low ripple voltage waveform. These encouraging results led to the development and field testing of a low frequency 3-phase precipitator power supply that was based on its single-phase predecessor.

LABORATORY TESTING OF PRECIPITATOR POWER SUPPLIES

In addition to modeling, laboratory testing was used to test a select group of precipitator power supplies. The goal of this testing was to confirm the results of the modeling and identify additional power supply characteristics that would be encountered in actual operation.

For laboratory testing, a test ESP was constructed which allowed for the entire mechanical configuration of the precipitator to be changed. For example, different discharge electrodes can be configured at various plate spacings, and precipitator problems like close clearances and tracking insulators can be introduced. For each test, the test ESP was equipped with one of three commercially available precipitator power supplies: single-phase, high frequency switch mode, and a low frequency 3-phase.

Table 5: Precipator Power Supply Modeling Results

Precipitator Power Supply Characteristics[1]

Power Supply	Low Ripple Output	Frequency	AC Line Input		DC Voltage and Current Output				Sparking	
			Power Factor	Total Harmonic Distortion (Input)	Ripple in Output Voltage[2]	Peak to Average Voltage Ratio	Ripple in Output Current[2]	Peak to Average Current Ratio	Total Harmonic Distortion (Output)[3]	Maximum Time to Spark Quench	Energy Delivered to Spark by Power Supply[4]
Single-Phase	No	Low	0.566	21.40%	11.80%	1.235	72.59%	2.132	0.97%	8.33×10^{-3} seconds	7.8×10^{-3} Joules < .1% of Total Spark Energy
Single Phase with External Filter[5]	Yes	Low	0.580	18.15%	2.39%	1.036	68.19%	1.883	0.75%	8.33×10^{-3} seconds	22.05×10^{-3} Joules < .1% of Total Spark Energy
Switch Mode - Phase Controlled	Yes	Medium	0.917	29.61%	1.68%	1.033	71.64%	2.281	40.21%	1.25×10^{-3} seconds	$\approx 8.53 \times 10^{-3}$ Joules < .1% of Total Spark Energy
Switch Mode - Amplitude Controlled	Yes	Medium	0.917	29.43%	1.35%	1.032	58.69%	2.050	44.25%	1.25×10^{-3} seconds	$\approx 4.17 \times 10^{-3}$ Joules < .1% of Total Spark Energy
Switch Mode - Frequency Controlled	Yes	High	0.926	35.17%	0.11%	1.002	122.55%	3.324	132.34%	30×10^{-6} seconds	55.7×10^{-6} Joules < .1% of Total Spark Energy
Switch Mode - Phase Controlled	Yes	High	0.914	36.25%	0.02%	1.000	48.57%	1.589	69.07%	60×10^{-6} seconds	70.9×10^{-6} Joules < .1% of Total Spark Energy
3-Phase	Yes	Low	0.826	13.01%	0.57%	1.009	10.45%	1.126	1.78%	5.55×10^{-3} seconds	5.7×10^{-3} Joules < .1% of Total Spark Energy
Perfect Power Supply[6]	Yes		1.000	0.00%	0.00%	1.000	0.00%	1.000	0.00%	0.00 seconds	0.00 Joules

[1] Modeled for power supply rated at 80 KV, 1000 mA, field capacitor 0.1 µF, field resistor 80KΩ.
[2] Percent Ripple (RMS of Ripple/Average Output)
[3] Harmonic frequency content above 1000 Hz
[4] Total spark energy = 320 Joules
[5] External filter .37 µf capacitor, 335Ω resistor
[6] Theoretical ideal data

An example of the laboratory testing is shown in Figure 12 and demonstrates the benefit of low ripple power supplies. Figure 12 shows the combined result of three tests, one for each power supply.

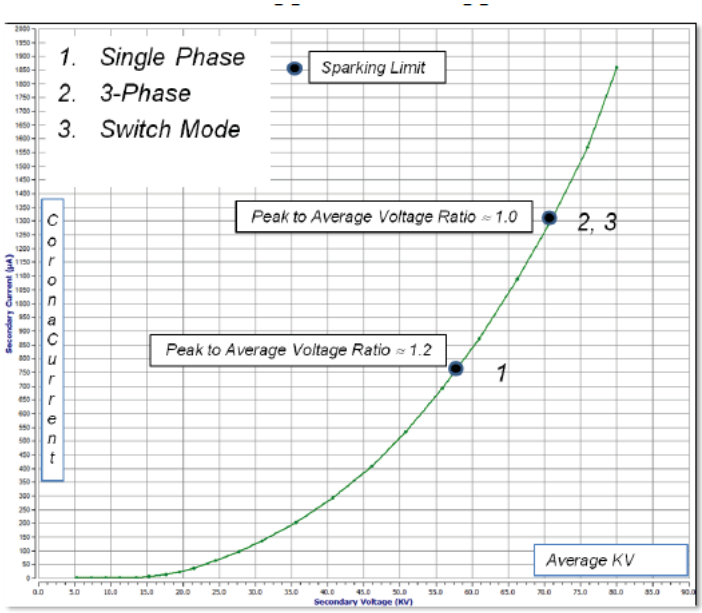

Figure 12: VI Curve for Single-Phase and Two Low Ripple Power Supplies

In each test, the power supply was operated from zero power to the point where sparking occurred and the typical average Voltage-Current (VI) curve plotted. It is interesting to note that the shape of the VI curve was established by the discharge electrode selected and the physical configuration of the test ESP. Therefore, all three power supplies tracked identically along the curve. In all three cases, precipitator sparking occurred at 71 kV which limited the power supply from going any higher. For the single-phase precipitator power supply (1), which is high ripple, when the peak voltage was 71 kV, the average voltage was 57 kV, which amounts to a peak-to-average-voltage ratio of about 1.2. For the 3-phase and high frequency switch mode precipitator power supplies (2, 3), which are both low ripple, when the peak voltage was 71 kV, the average voltage was very near 71 kV, which amounts to a peak-to-average-voltage ratio of 1.0. The ability to gain that much average voltage produces a substantial increase in the average current. The net result is more corona power into the ESP. A reduction in the peak-to-average-voltage ratio from 1.2 to 1.0 results in a 20% increase in voltage. This amount of voltage increase tracking a typical VI curve can produce up to 35% more average current.

SPARK DELAY, ENERGY AND QUENCH

When a spark occurs, it dissipates all of the energy stored in the precipitator field and the spark extinguishes. In response to the spark, the power supply quenches or turns off for a period of time, and then reapplies power to re-charge the precipitator field. However, the power supply does not turn off the instant the spark occurs. There is a delay based on the type of power supply, and during this delay, energy is delivered to the spark from the power supply. Table 5 shows the delay period and the amount of energy delivered to the spark during the delay for various power supplies. Each power supply type analyzed delivers less than 0.1% of the total spark energy.

The majority of energy (>99.9%) dissipated by the spark comes from the energy stored in the capacitance of the precipitator field and not the power supply as shown in the following analysis:

The capacitor comprised by the precipitator field stores energy in the form of an electric field. As discussed previously, the size of the capacitor is approximately 10 nf per milliamp of power supply and for a 1000 milliamp power supply, this would be approximately 0.1 µf. This is not an insignificant amount of capacitance. The amount of energy (measured in joules) stored by the field capacitance is given by:

Equation 1. $W = 0.5*C*V^2$
where:
W = energy stored (joules)
C = capacitance (farads)
V = voltage (volts)

For the precipitator field with a capacitance of 0.1 µf, operating at 45 kV, there are 101 joules stored in the capacitive field which will be dissipated at spark. Therefore, referring to Table 5, the energy delivered to the spark by each power supply is much less than 0.1% of the total energy dissipated by the spark.

We can also calculate the power in a spark. If we take the earlier example and assume the spark will dissipate the 101 joules of stored precipitator field energy in 1 millisecond, then we have the following:

Equation 2. $P = dW/dt$
where:
P = power (watts)
dW = change in energy (joules)
dt = change in time (seconds)

This yields 101,000 watts. In an internal BHA study conducted in 2002, an actual measurement made of the spark current on an operating precipitator field was on the order of 22,000 amperes. This precipitator field had rigid discharge electrodes, 16 in. wide gas passages, a single-phase power supply rated at 70 kV, 750 mA and controlled by an SQ-300® automatic voltage control. This energy output occurs over a very short period of time and at least partially explains why repeated sparking in the same location can cause damage, such as wire breakage in a weighted wire precipitator.

In summary, the amount of energy delivered by each power supply to the spark is proportionally very small. Care should always be exercised with large precipitator fields (which increase capacitance) and wide plate spacing (which increases voltage) since spark energy is directly proportional to the capacitance and the square of the voltage.

HARMONICS AND TOTAL HARMONIC DISTORTION

Precipitator power supplies connect to the power line and draw power not only at the fundamental frequency but at harmonic frequencies which are whole number multiples of the fundamental frequency. This non-linear load causes distortion of the input waveform and can cause many problems in the electrical distribution system including heating of conductors, nuisance breaker trips, and interference with other plant equipment. It is therefore important to have a measurement of how much distortion exists for each power supply type. One widely accepted measurement is total harmonic distortion (THD) which is a summation of all of the harmonics present in the system. The modeling data in Table 1 shows that the low frequency designs exhibit the lowest input THD and can therefore be expected to provide significantly fewer installation and maintenance problems due to harmonics. In addition, the power factor for each power supply type is also shown.

Precipitator power supplies also produce harmonics at the output. The DC waveform is made up of many frequencies including a fundamental frequency and its harmonics. This is particularly troubling in precipitator power supplies because ground is a current-carrying power lead and is therefore energized with harmonic frequencies. Since all of the plant equipment and the neighboring facilities plant equipment are connected through ground, the potential exists to cause interference with other plant equipment, including other precipitator power supplies. This is particularly true as radiated RF emissions increase with frequency.

Some of the known problems with high THD at the output are equipment failure, heating of conductors, crosstalk between power supplies, and interference with other plant equipment. In actual practice, these types of problems are often difficult to identify and solve and they are often specific to the location as well. To predict the likelihood of encountering these types of problems, a measurement of how much distortion exists in the output DC waveform is useful. THD can be used here as well. The output THD for each power supply type is shown in Table 5. In this case, the THD is calculated for frequencies above 1000 hertz. Again, the low frequency designs exhibit the lowest output THD and can be expected to encounter fewer problems in this area. To overcome some of these difficulties when applying high frequency designs, manufacturers provide detailed bonding and grounding specifications which must be meticulously followed.

The internal electrical connections inside the precipitator are also an area of concern. Historically, the precipitator was constructed for low frequency operation with connections being bolted together or using a friction fit. Both of these connection types may be inadequate for high frequency operation[11] leading to voltage drops at the connections, both in the high voltage distribution system and the ground system. A particularly interesting problem occurs when the voltage drop in the internal ground connection causes crosstalk and interference between precipitator power supplies. This can be very difficult to troubleshoot and correct without addressing the internal connections of the precipitator. Experience has shown that for a given installation, it is difficult to predict if the internal connections will be a concern when converting to high frequency power supplies. A generalization would be the higher the frequency, the more one would expect problems. This generalization has been experienced in the industry where some power supplies are trouble-free and others experience problems, but it is often site-specific.

APPLICATION DATA - LOCATION, SIZE, WEIGHT, AND FOOTPRINT

Electrical performance discussed previously is a very important consideration in the selection of a precipitator power supply. Perhaps as important, however, is its physical configuration. Table 6 shows the physical characteristics for four commercially available, roof-mounted precipitator power supplies. The differences are significant.

The high frequency power supply designs shown are integrated units, meaning the entire power supply is contained in one package. This is a necessary configuration since it

Table 6: Comparison of Four Preciptator Power Supplies

Comparison of Four Commercially Available Roof-Mounted Precipitator Power Supplies in Different KWs

Power Supply	Low Ripple Output	Frequency	External Control Cabinet	CLR Included in TR Set[1]	Cost Comparison[2]	Footprint on Roof (Sq Ft)	Footprint Comparison[3]	Weight on Roof (Lbs)	Weight Comparison[4]	Cooling on Roof
SMPS(1) 21 KW	Yes	High	No	-	1.49	14.15	0.66	1,050	0.56	Fan
SMPS(2) 20 KW	Yes	High	No	-	1.78	8.37	0.39	528	0.28	Pump & Fan
3 Phase 24 KW	Yes	Low	Yes	Yes	1.16	28.51	1.33	3,527	1.88	Passive
Single Phase 24 KW	No	Low	Yes	Yes	1.00	21.43	1.00	1,874	1.00	Passive
SMPS(1) 35 KW	Yes	High	No	-	1.89	13.81	0.64	1,200	0.64	Fan
SMPS(2) 28 KW	Yes	High	No	-	1.76	8.37	0.39	528	0.28	Pump & Fan
3 Phase 32 KW	Yes	Low	Yes	Yes	1.16	28.51	1.33	3,638	1.94	Passive
Single Phase 32 KW	No	Low	Yes	Yes	1.00	21.43	1.00	1,874	1.00	Passive
SMPS(1) 70 KW	Yes	High	No	-	2.31	15.33	0.65	1,300	0.46	Oil Circulator & Fan
SMPS(2) 60 KW	Yes	High	No	-	1.70	8.37	0.35	528	0.19	Pump & Fan
3 Phase 72 KW	Yes	Low	Yes	Yes	1.17	31.02	1.31	3,968	1.41	Passive
Single Phase 72 KW	No	Low	Yes	Yes	1.00	23.73	1.00	2,822	1.00	Passive
SMPS(1) 120 KW	Yes	High	No	-	2.31	22.23	0.86	2,300	0.65	Oil Circulator & Fan
SMPS(2) 120 KW	Yes	High	No	-	2.22	11.83	0.46	1,100	0.31	Pump & Fan
3 Phase 120 KW	Yes	Low	Yes	Yes	1.12	37.55	1.45	5,071	1.44	Passive
Single Phase 120 KW	No	Low	Yes	Yes	1.00	25.83	1.00	3,527	1.00	Passive

[1] The Current Limiting Reactor (CLR) is applicable only to 3-phase and single phase. Locating the CLR in the TR set increases its footprint and weight. The CLR can be located remotely.

[2] Within each size, the cost of SMPS(1), SMPS(2), and 3-phase is compared to single phase. For Single Phase and 3-Phase, cost includes external control cabinet and CLR in TR set.

[3] Within each size, the footprint of SMPS(1), SMPS(2), and 3-phase is compared to single phase. For Single Phase and 3-Phase, the footprint excludes the external control cabinet.

[4] Within each size, the weight of SMPS(1), SMPS(2), and 3-phase is compared to single phase. For Single Phase and 3-Phase, the weight excludes the external control cabinet.

would be quite difficult to separate the transformer and electronics with high frequency. Having an integrated unit is a very convenient and efficient design with all of the power supply components located in one place. The power supply is packaged as a complete assembly instead of individual components that must be connected together.

The high frequency power supply designs are also physically smaller and lighter. The high frequency power supply designs utilize active cooling which helps achieve the smaller size and weight. This can become very important when trying to fit equipment on a crowded precipitator roof that has a limited ability to carry additional load.

However, there are some disadvantages to this configuration. An integrated unit often means the sensitive electronics are located in a harsh environment. This directly affects the reliability of the power supply, and having personnel service equipment in this environment is less than ideal. In addition, active cooling is another system which must be maintained, with additional energy required to operate these systems. Finally, an integrated unit means there is one source of supply for parts and service which can cause significant service interruptions if there are problems.

The low frequency power supply designs shown in Table 6 are not integrated but have separate control cabinets. This is possible with low frequency designs since standard electrical wiring can be used to connect components. The separate control cabinet allows the high voltage transformer to be located on the roof while the control electronics are located remotely, often in an environmentally controlled room. This configuration has been successfully used for many years with the single-phase power supply. The low frequency power supply designs are physically larger and heavier. They utilize passive cooling for the transformer which eliminates the need to supply and maintain an additional cooling system. Lastly, separating the controls and transformer allows each component to be sourced from multiple suppliers which helps assure a continuous supply.

There are also disadvantages to this configuration. As previously discussed, it is sometimes a challenge to find a suitable location for equipment that is larger and heavier. To solve this problem, the power supply can be located away from the main precipitator structure and then connected by means of high voltage cable. In addition, there is wiring and cabling between components which must be considered.

COST

Cost is also a significant consideration in the selection process of precipitator power supplies. Table 6 shows the comparative cost of four commercially available, roof-mounted precipitator power supplies and again, the differences are significant. The cost shown is the capital cost, or the cost to purchase the entire power supply. For the sake of comparison in Table 6, within each kW size range, the cost of the single-phase power supply was set to 1.00. The cost of the other three power supplies was then compared to the single phase. As can be seen, as the kW size increases, the differences in cost increase as well.

High frequency power supply designs are more expensive. However, since they are integrated, there is less field wiring, and installation cost should therefore, be less than the low frequency power supply designs. On the other hand, due to the combination of environment, high frequency and active cooling, maintenance cost is expected to be more than the low frequency power supply designs.

Low frequency power supply designs are less expensive. However, since they are separate components which must be connected in the field, the wiring and installation cost should be more than the high frequency power supply designs. Since they operate at a lower frequency, have passive cooling, and the electronics are in a protected environment, the maintenance cost should be less than the high frequency power supply designs.

RELIABILITY

The predicted reliability is the most difficult parameter to quantify. It is well known and accepted that the reliability of the single-phase precipitator power supply is excellent. There are many cases of this type of power supply operating continuously for more than 40 years. This is a reliability benchmark that one would like to duplicate with low ripple power supply designs.

Anecdotal evidence has shown that high frequency power supplies have had a poor reliability record, although it has improved in recent years. They suffer from such challenging factors as operating at high frequencies while connected to a device designed for low frequency (precipitator), significant internal heating, active cooling systems, harsh environment, radio frequency interference and harmonics. All of these factors have contributed to reliability issues. Suppliers have made changes over the years in an attempt to address each issue with varying degrees of success. Current experience indicates that additional effort is needed to equal the reliability of a single-phase power supply.

One of the goals of field testing the low frequency 3-phase power supply was to evaluate reliability. The results to date are promising; there have been no failures of the 3-phase power supply during the six-month test run. The results were somewhat expected considering the 3-phase is basically an extension of the single-phase power supply design which has an excellent reliability record, and the modeling and lab testing results support this.

FIELD TESTING OF SINGLE-PHASE AND 3-PHASE POWER SUPPLY AND OPERATING CONDITION OF THE ESP

The ESP used for performing the 3-phase power supply test is on a tangentially-fired boiler. It burns coal with a sulfur content of 1.9 lb/MBtu, has no selective catalytic reduction (SCR) system and no scrubber. The ESP consists of two boxes with rigid discharge electrodes and 16 in. wide gas passages. There are 4 fields (each 12 ft x 50 ft), and there are 8 TR sets per box (2 x 4 matrixes). Fields 1 and 2 have 70 kV, 750 mA conventional TR sets; fields 3 and 4 have 70 kV, 1000 mA sets. All TR sets are controlled by B&W SQ-300® automatic voltage controls. On the "A" box, the inlet field 1A-1 TR set was replaced with a 480 V, 109 A, 90 kV, 900 mA, 3-phase TR set for the purpose of testing.

The results obtained when comparing the operating power levels of the test 3-phase power supply and the conventional power supply are shown in Figure 13.

As shown in Figure 13, the 3-phase power supply typically produced ESP kW values 1.5 times that of the conventional power supply (as determined by the average 3-phase power/ average single-phase power). This field test confirmed the results of the laboratory testing which indicated that low ripple power supplies are expected to provide more precipitator field power. A significant impact on opacity was not anticipated because the test only involved 1/16th of the ESP.

Conditions at the field test site and the operation of the low frequency 3-phase power supply that has been installed continue to be monitored. More tests will be run at varied precipitator loads.

SUMMARY

A systematic study was performed using electrical modeling, laboratory tests, and field tests to determine the advantages and disadvantages of the many types of ESP power supplies. The results show that:

- A 3-phase low frequency precipitator power supply was developed and field tested as a result of this study to overcome many of the deficiencies discovered in the analysis of precipitator power supplies.

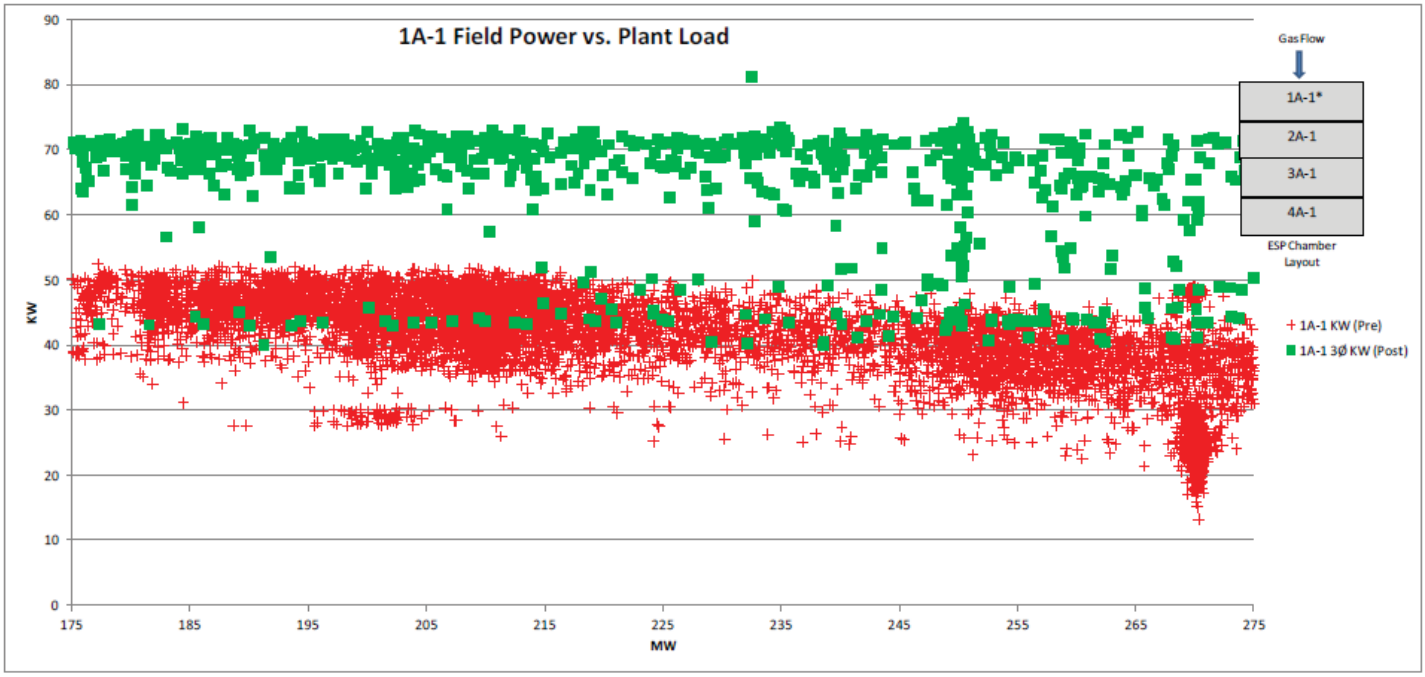

Figure 13: MW vs. kW (Pre and Post 3-Phase Install)

- The increase in corona power from a low ripple power supply can be achieved with several different technologies (SMPS, 3-phase low frequency, mid-frequency).
- Modeling data showed that the energy delivered by the precipitator power supply to the spark was insignificant compared to the total energy dissipated by the spark.
- Harmonics are unwanted and have been shown to be a concern on both the input and output of the precipitator power supply. Low frequency designs (including the 3-phase) produce fewer harmonics.
- Integrating all components into one package has the advantage of the most compact configuration. This can have the disadvantage of placing the power supply in a harsh environment which affects service life and maintenance and restricts the user to a single source of supply.
- Providing a separate transformer and control cabinet has the advantage of placing the electronic controls in a controlled environment and allows for duplicate sources of supply. This has the disadvantage of the need for a remote control cabinet and larger size and weight.
- Low frequency power supply designs (including the 3-phase) use passive cooling while high frequency power supply designs require active cooling. The increase in components and complexity for active cooling increase cost and maintenance.
- High frequency precipitator power supply designs provide low ripple at higher cost, lower reliability, but in a smaller, lighter integrated package.
- Low frequency precipitator power supply designs (including the 3-phase) provide low ripple at lower cost, higher reliability, but in a larger, heavier package with a separate control cabinet.
- The 3-phase and high frequency switch mode precipitator power supplies provide the lowest ripple voltage on an ESP load.
- The field test showed the 3-phase precipitator power supply produced an average 50% higher power in the ESP compared to the single-phase precipitator power supply. This suggests that like other low ripple power supplies, the 3-phase power supply can produce higher ESP collection efficiencies.

REFERENCES

1. Hall, H. J., Critical Electrostatic Precipitator Technology Factors for Very Fine Particle Collection, 3rd International Conference on Electrostatic Precipitation, October 1987, Padova, Italy.
2. White, H. J., Review of the State of Technology, International Conference on Electrostatic Precipitation, Monterey, CA, October 1981.
3. Kumar, K.S., Knapik, J.A., and Hartman, D.S., Electrostatic Precipitator Upgrade Opportunities through a Review of Best Performers in Coal-fired Power Plants, 2012 Power Plant Pollutant Control "MEGA" Symposium, Baltimore, MD, August 2012.
4. Hall, H. J., Automatic Voltage Control System Based on Optimum Average Spark Rate, U.S. Patent 2,623,608, 1952.
5. Lloyd, D. A., Electrostatic Precipitator Handbook, pg. 49, Adam Hilger, Bristol, England, 1988.
6. .Johnston, D.F., Method and Apparatus for Controlling Power to an Electronic Precipitator, U.S. Patent 4,605,424, August 12, 1986.
7. .Johnston, D.F., Electronic Precipitator Control, U.S. Patent 4,860,149, August 22, 1989.
8. .Johnston, D.F. et al, Electrical Control System for Electrostatic Precipitator, U.S. Patent 5,068,811, November 26, 1991.
9. .Johnston, D.F. et al, Apparatus and Method for Filtering Voltage for an Electrostatic Precipitator, U.S. Patent 6,611,440 B1, August 26, 2003.
10. .Johnston, D.F. et al, Apparatus and Method for Filtering Voltage for an Electrostatic Precipitator, U.S. Patent 6,839,251 B2, January 4, 2005.
11. Van Dijk, P., Critical Aspects of Electrical Connector Contacts, Proceedings 21st International Conference on Electrical Contacts (ICEC), Zurich, 2002.

Disclaimer

Although the information presented in this work is believed to be reliable, this work is published with the understanding that Babcock & Wilcox (B&W) and the authors and contributors to this work are supplying general information and are not attempting to render or provide engineering or professional services. Neither B&W nor any of its employees make any warranty, guarantee or representation, whether expressed or implied, with respect to the accuracy, completeness or usefulness of any information, product, process, method or apparatus discussed in this work, including warranties of merchantability and fitness for a particular or intended purpose. Neither B&W nor any of its officers, directors or employees shall be liable for any losses or damages with respect to or resulting from the use of, or the inability to use, any information, product, process, method or apparatus discussed in this work.

For further information contact
David F. Johnston at dfjohnston@babcock.com

Is a bi-annual newsletter sponsored by and for the Worldwide Pollution Control Association
www.wpca.info

Purpose

To foster new ideas and greater awareness concerning pollution control in the energy industry

Publisher

Reinhold Environmental Ltd.

Comments & Other Inquiries to:

Reinhold Environmental
3850 Bordeaux Drive
Northbrook, IL 60062 USA
1.847.291.7396
sreinhold@reinholdenvironmental.com

For more information on the WPCA Please visit our website at
www.wpca.info

Acid Gas Control Technologies

Challenges of Retrofitting Dry / Semi-Dry Scrubbing Technologies

Written by Kevin Cosman, Process Engineer, KC Cottrell Inc

BACKGROUND

As the requirements for acid gas control on combustion boilers become more stringent, the strain put on both existing and new technologies becomes more demanding. Compliance with the MATS, MACT, CSAPR or other regulations has led every site in the United States to reevaluate their current technologies and created a need to look forward. With the decreasing operating margin of error on power boilers, specific advancements have been necessitated in the area of operational and maintenance costs for all flue gas desulfurization products. Multipollutant control technologies are used to remove acid gases, specifically focusing on SO_2 and HCl. With a variety of technologies currently available to end users, a company must be even more vigilant in understanding the pros and cons to each type of technology in today's marketplace. Specific considerations must be made when simultaneously trying to reuse existing equipment and retrofitting new technologies.

DRY FGD CHEMISTRY

Different sorbents may be available depending on what technology is selected. Most commonly used include calcium or sodium based sorbents.

At low temperatures, in order for calcium sorbents to be reactive, they must be hydrated from their original form of quicklime (calcium oxide, CaO) to calcium hydroxide (hydrated lime, $Ca(OH)_2$). The chemical reactions of calcium sorbents include:

$$Ca(OH)_2 + 2HCl \rightarrow CaCl_2 + 2H_2O$$

$$Ca(OH)_2 + SO_2 \rightarrow CaSO_3 + H_2O$$

The hydration process can take place either on site or off, depending on the type of equipment the site has installed (slaker, hydrator). This process can be difficult to handle, so many sites are looking to purchase pre-hydrated lime. The effective resistivity of the ash will increase (how much will depend on lime injection rates), so if an electrostatic precipitator (ESP) is downstream of a calcium based system, particulate emission control may be affected in a negative manner.

Sodium based sorbents have been found to be effective in FGD systems, but have their own set of rules compared to other sorbents. These sorbents may include Sodium Bicarbonate ($NaHCO_3$) or Trona ($Na_2CO_3 \cdot NaHCO_3$) and their reaction chemistry can be seen below:

$$Na_2CO_3 + SO_2 \rightarrow Na_2SO_3 + CO_2$$

$$Na_2CO_3 + SO_3 \rightarrow Na_2SO_4 + CO_2$$

$$Na_2CO_3 + 2HCl \rightarrow 2NaCl + H_2O + CO_2$$

Sodium sorbents will be beneficial to an ESP with regards to fly ash resistivity, however some ash disposal issues have been found to occur, specifically leeching of sodium compounds into ground water.

Other types of proprietary sorbents may be commercially available also. No matter what type of sorbent is used, extra particles will be added to the system, affecting the downstream particulate control device.

TYPES OF FGD EQUIPMENT

Each general category of dry FGD equipment has its own benefits as well as disadvantages when it comes to initial capital investment or long term operating costs. The lowest capital investment system would be a simple Dry Sorbent Injection system (DSI). This would be a simple skid of a nozzle/lance integration that would pneumatically inject a dry sorbent of the user's choosing directly into the duct. Because it is a once through system with no flue gas temperature modification or sorbent recirculation, high sorbent consumption values can be expected in the range of 2~5 for a stoichiometric ratio of calcium to inlet sulfur. This will lead to high operating and sorbent costs, as well as restricting your ultimate removal rates to <70% of inlet values for SO_2. If a sodium based sorbent is used, higher removal efficiencies can be achieved however lack of species selectivity between SO_2 and HCl can lead to high stoichiometry.

Another type system having many decades of commercial operations is a Spray Dryer Absorber (SDA). These will use a large reactor vessel (>30' in diameter) with hydrated lime being injected as slurry with water through a rotary or other

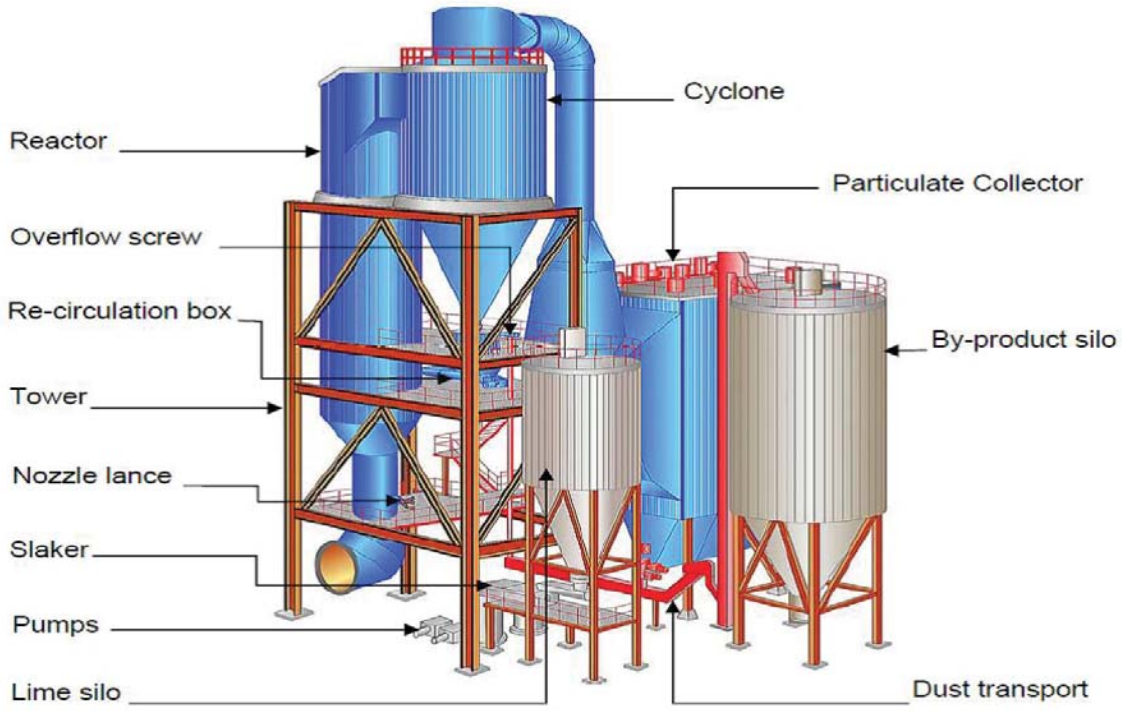

Figure 14: Gas Suspension Absorber Arrangement

type of atomizer. Residence time in the vessels can be as high as 12-15 seconds. The temperature modification with water injection positively affects the apparent stoichiometry however fly ash recycle systems installed to get high sorbent utilization, as the system has no ash internal recycle. Also, SDA systems generally require onsite slaking.

The third general type of system available is known as circulating dry scrubber (CDS). The reaction chemistry is similar to that of SDAs, however these systems will use internal ash recycle from a particulate collector (often via air-slides from an elevated collector) to get high sorbent utilization. Often times these reactors will have much lower residence times (3-5 seconds). Sorbent injection is typically pneumatic however the use of pressure nozzles (as opposed to rotary atomizers) for water injection.

CHALLENGES OF FGD RETROFIT

At each particular plant there are sets of unique challenges when new equipment is looking to be retrofitted. Often times, footprint issues are the largest obstacle facing plants. The optimal location to locate new equipment, and how to reroute the ducting become difficult questions to answer with large equipment being required. Large reactor vessels can be problematic to find room for in a frequently tight plant layout.

Most types of CDS designs require an elevated particulate control device to allow for easier recirculation of reagent and byproduct through means of air-slides or other material handling technologies. Also, the filter is typically large in size due to the very high inlet loading. The necessity for an elevated particulate control device is dictated by the use of air slides or other gravity-type recycle systems from the fabric filter. Additional loading to the new/updated fabric filter decreases bag life due to increased cleaning frequency and wear. These significant changes lead to large capital investment requirements, additional maintenance costs and operational downtime due to high levels of construction.

ALTERNATE RECIRCULATION TECHNOLOGIES

An alternate approach to CDS recirculation is called the Gas Suspension Absorber (GSA). This technology offers a similar system to other CDS types however it integrates cyclones in between the small scrubbing vessel and the particulate control device. A diagram can be seen in Figure 14 (above) which portrays how the GSA is configured.

FINAL THOUGHTS

Although retrofitting any existing facility has its challenges, there are various types of equipment in the current market that allow you to come into compliance the MATS or MACT rules. Site specific conditions will dictate the proper choice of equipment for any particular plant. Table 7 (page 20) offers a basic comparative to summarize the differences, both material and commercial, of the various categories.

Table 7: Summary of Each Technology's Retrofit Attributes

System Type	Lime Sorbent Utilization	Retrofit Capital Costs	Future Operating Costs	Dry or Wet Injection	Vessel Footprint	Keep Existing Particulate Device w/o Modification
DSI	LOW	LOW	HIGH	DRY	N/A	SOMETIMES
SDA	MEDIUM	HIGH	MEDIUM	WET	LARGEST	SOMETIMES
CDS	HIGH	MEDIUM	LOW	MOSTLY DRY	MEDIUM	RARELY
GSA	HIGH	MEDIUM	LOW	EITHER	SMALLEST	FREQUENTLY

For further Information contact
Kevin Cosman at kcosman@kccottrell.us

Mr. Kevin Cosman is a process engineer for KC Cottrell Inc out of their Flemington, NJ office. He has been heavily involved in the design of a variety of air pollution control technologies with KC Cottrell's world wide solutions team including ESPs, Fabric Filters, SCRs, and Scrubbers. He is a graduate of Rutgers University with a B.S. in Chemical Engineering

KC Cottrell Inc.

The Use of Flue Gas Mixing Technology for Improving In-Duct Sorbent Injection System Performance

By Matthew Quitadamo, Babcock Power Environmental Inc.

Introduction

Dry sorbent injection systems for utility coal-fired generation units have been around for decades. However, they have grown in popularity over the last five to 10 years due to recent regulatory drivers such as the Mercury and Air Toxics Standard (MATS) and the Cross-State Air Pollution Rule (CSAPR) and their lower capital cost, space requirement, and lead times as compared to traditional treatment technologies (i.e. wet and semi-dry scrubbers).

As the name suggests, dry sorbent injection is a process of injecting powdered/pulverized sorbent into a duct or furnace to capture contaminants, typically acid gases (i.e. SO_2, SO_3, or HCl) or mercury. Most systems today use hydrated lime, trona, or sodium bicarbonate for the reduction of acid gases or activated carbon or amended silicates for the reduction of mercury species. The choice of sorbent depends on the type of pollutant, removal efficiency required, and system operating cost.

The effectiveness of a dry sorbent injection system depends on several factors, such as sorbent properties, choice of injection location, type of particulate control device, and injection system design. Of these factors, injection system design, or more specifically improving sorbent mixing/dispersion, has been a major focus for those involved with the design and operation of these systems.

Throughout the 1980's and into the early 1990's, the Department of Energy (DOE) funded a program which provided a single in-depth study in this field [1]. The program examined a broad range of processes, sorbents, injection locations, and methods. As a result, it was concluded that the chemistry was understood for the different sorbents and that "proper mixing and dispersion of the injected sorbent into the temperature window required for maximum removal are more important than finding the optimum injection level or temperature [2]." More recent literature [3, 4, 5, 6, 7] has reinforced this concept. In some cases, reported improvements in pollutant capture efficiency are as much as 10% to 30% due to improved sorbent dispersion [8, 9, 10].

Conventional Approaches for Optimal Coverage and Dispersion

Conventional approaches for optimizing dispersion and coverage rely heavily on the injection grid layout. According to Gentry [11], optimal designs should utilize one injection per every 40 to 45 square feet of duct cross-section and maintain a layout aspect ratio close to unity (H/W $\cong$ 1.0). Typically this requires a high density of injection points, and in turn, small lance diameters to maintain acceptable transport line design parameters. As a result, conventional systems are prone to pluggage and poor sorbent dispersion within the flue gas. In some instances, it is possible to take advantage of the inherent turbulence at or near the injection location to promote better sorbent dispersion, but this varies greatly from one system to the next and is not always feasible.

Static Mixers for Sorbent Injection

One approach for improving the dispersion of sorbent is to induce turbulence to promote mixing. This is accomplished by utilizing static mixers within the flue gas duct. Static mixers create vortices that enhance gas-solids mixing and have been used in several utility applications including SCR's, upstream ESP's, and throughout flue gas duct work to promote uniformity for temperature, velocity, and concentration profiles.

When using static mixers for sorbent injection, it is possible to provide near instantaneous mixing at the point of injection, maintain consistent sorbent coverage over the entire load range, and even improve capture efficiency and/or sorbent consumption. As a result, systems with static mixers can often reduce the number of injection lances required,

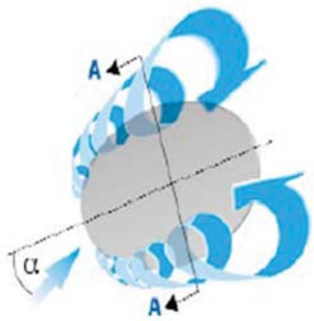

Figure 15: Leading-edge vortices at a circular static mixer plate [12]

thereby allowing for larger lance diameters as compared to conventional lance designs. These items will be covered in greater detail over the next few sections.

Sorbent Dispersion and Coverage

As previously mentioned, conventional sorbent injection systems make use of multiple lances positioned at different insertion depths within the duct in order to provide adequate gas-solid contact for sorption to occur. Without turbulence, the sorbent tends to mimic flue gas flow forming slowly, expanding bands or plumes. On the other hand, static mixer sorbent injection systems disperse solids across the entire cross-sectional area of the duct in a relatively short distance after being released. Results from computation fluid dynamic analysis for a single injection lance, both with and without static mixing, have been included in Figures 16 and 17 to better illustrate typical sorbent behavior.

The simple injection lance design without static mixing (Figure 17) resulted in inefficient mixing and as a result incomplete coverage across the duct cross-section. Alternatively, the combination of a single lance with a dedicated static mixer plate (Figure 16) provided nearly complete coverage within a short distance downstream of the injection point.

Generalizing these results, the use of static mixers can provide faster dispersion and better sorbent coverage. These generalizations become more important when considering the injection of sorbent across a large cross-sectional area, especially when there is little to no inherent turbulence to promoted dispersion.

As an example, Figures 18 and 19 (page 23) illustrate sorbent behavior both with and without static mixers for a full-scale injection system. For the scenario presented, sorbent is injected into the duct just downstream of an SCR reactor, where there is little inherent turbulence introduced to the system.

As shown, the particle trajectories for the conventional injection system (without mixers) exhibit very poor dispersion throughout the duct, whereas the injection system with static mixers has superior dispersion and as a result almost complete coverage. It is also worth noting that the system including static mixers utilized fewer injection points: 8 injections with static mixers and 12 without.

Figure 19 suggests that the conventional injection system would require significantly more injection points to provide comparable coverage to that of the system utilizing static

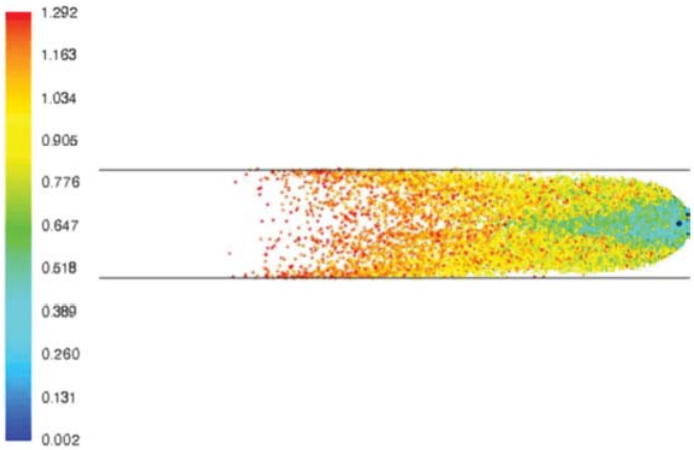

Figure 16: Particle Trajectories (colored by residence time, [s]) for a Single Injection Lance System with Statis Mixing.

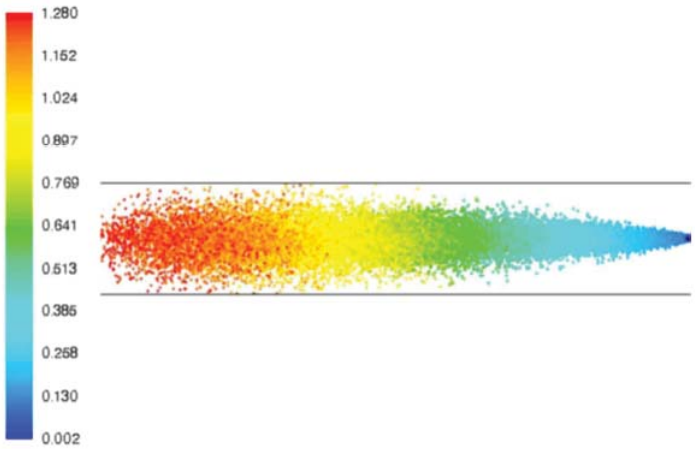

Figure 17: Particle Trajectories (colored by residence time, [s]) for a Single Injection Lance System without Statis Mixing.

mixers. While actual injection grid design is dependent on multiple factors (e.g. duct layout, duct dimensions, type of mixer), the use of static mixers typically reduces the number of the injection lances needed by half of what would be considered optimal for a conventional sorbent injection system.

Sorbent Coverage at Different Loads

Another benefit that can be attributed to the use static mixers for sorbent injection is consistent hydrodynamic behavior across all operating loads. As can be observed from Figure 20, (page 24) which represents the same single injection lance system that was already presented in Figures 16 and 17, the conventional system experiences varying patterns of coverage depending on the unit load. For the conditions examined, the sorbent plume starts closer to the duct wall and shifts towards the duct center as load decreases for the given system. It can also be noticed that the majority of sorbent

concentration profiles exhibit incomplete coverage, even at the outlet terminal location. Alternatively, the same single injection system coupled with a dedicated static mixer disc displays more consistent coverage as load varies. As illustrated, sorbent coverage remains relatively unchanged as unit load is reduced.

Capture Efficiency and Sorbent Consumption

At this point, we have established the benefits for using static mixers for sorbent injection with regards to coverage and dispersion. Well, so what? What does it mean with regard to performance?

As in-duct sorbent injection is a sorption process, gas-solid contact is critical to achieve high pollutant capture efficiency. Poor sorbent dispersion, and in turn incomplete sorbent coverage, will result in some pollutant passing through the duct untreated and thereby limiting the maximum achievable reduction.

As an example, Figures 21 and 22 (page 24) summarize two separate testing efforts at a 150 MW full-scale sorbent injection installation: one without static mixers and one with static mixers. For this system, hydrated lime was injected just after the economizer exit and collected in a downstream fabric filter. Results for both SO_2 and HCl capture vs. normalized stoichiometric ratio for total acid gases (NSR_T) are shown, where NSR_T is the operating stoichiometric ratio divided by the theoretical stoichiometric ratio.

NSR_T can be calculated as follows [13]:
Where F is the actual sorbent injection rate; X_i is the actual acid gas species flow rates in flue gas; β_i is the stoichiometric required sorbent to neutralize the acid gas species X_i.

Testing conducted without the use of static mixers is illustrated by the blue trend line and testing with static mixers is illustrated by the red trend line. As shown, there is a notable area of improvement for both contaminants when static mixers were used.

On that basis, there are two ways this improvement can be taken advantage of. The first, reduce sorbent usage. This is beneficial when designing new systems, especially those that include marginal particulate collection devices. Alternatively, results show that static mixers could also be used to improve system performance for a given sorbent feed rate. This could be beneficial for existing systems that need to perform at reduced emission limits. Either way, a significant improvement was realized.

$$NSR_T = \frac{F}{\sum(X_i \cdot \beta_i)}$$

Conclusion

Dispersion is critical to in-duct dry sorbent injection applications. Static mixers, which have been success-fully applied to several utility applications, are an effective way to improve dispersion for these systems. Use of static mixers can result in fewer, larger injection lances required, improved sorbent coverage throughout the system, consistent coverage across the full range of operating conditions, and improved emissions reduction and/or reduced sorbent consumption.

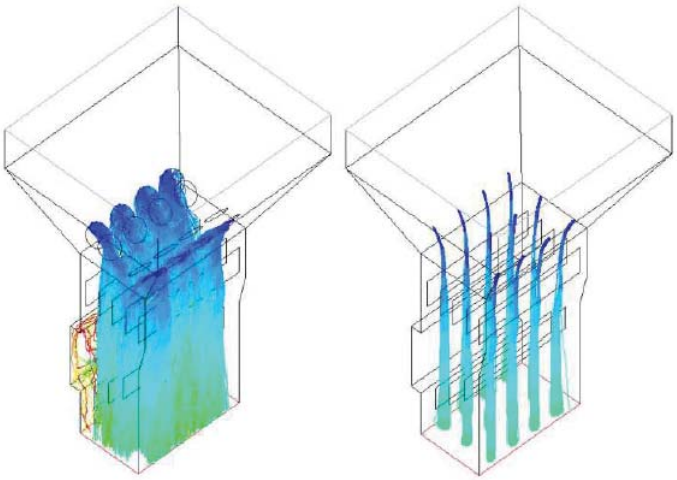

Figure 18: Particle Trajectories (colored by residence time) with and without Static Mixing

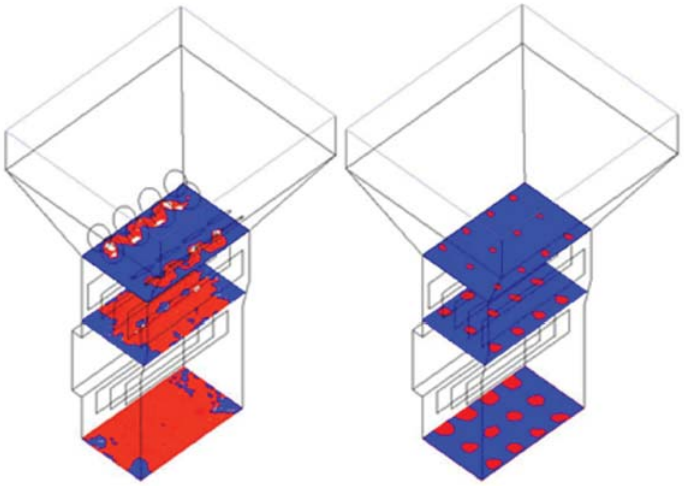

Figure 19: Sorbent Coverage (red = some sorbent, blue = no sorbent) with and without Static Mixing

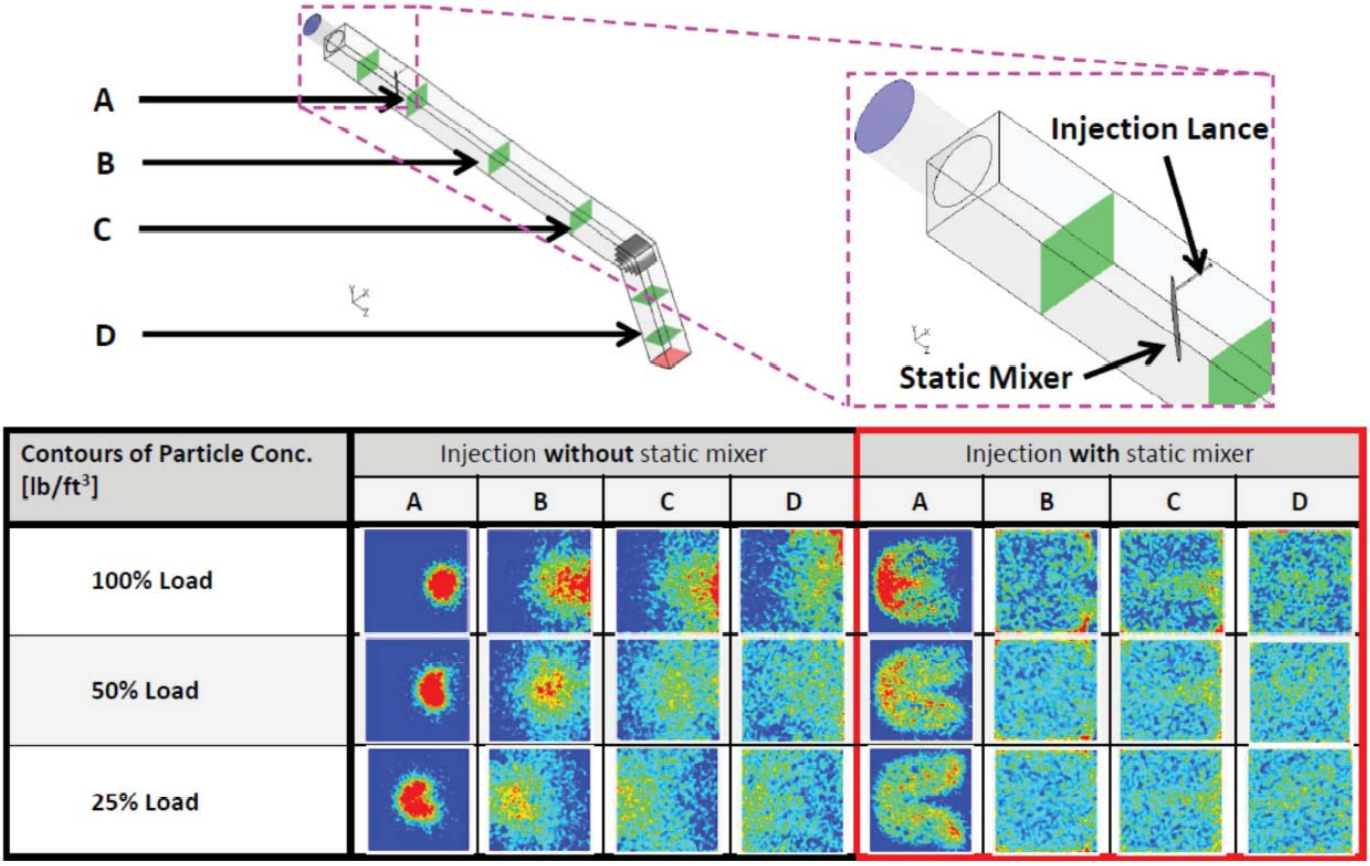

Figure 20: Sorbent Dispersion vs. Load for Both Conventional and Static Mixer Sorbent Injection System Designs.

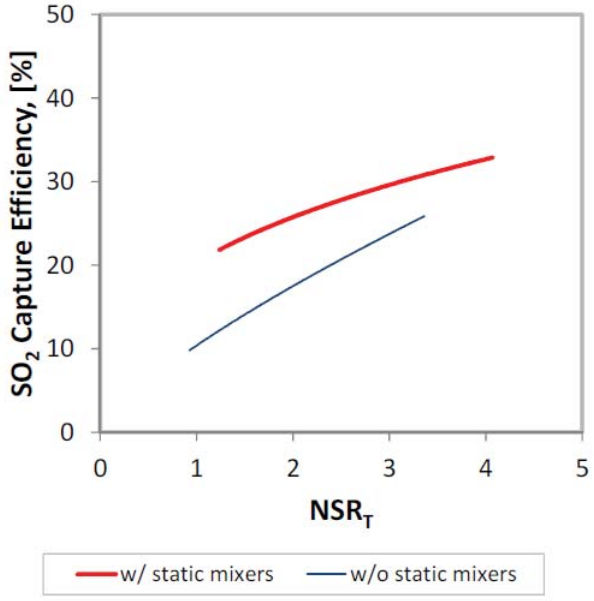

Figure 21: SO_2 Capture vs. NSR Test Data for Full-scale Sorbent Injection System.

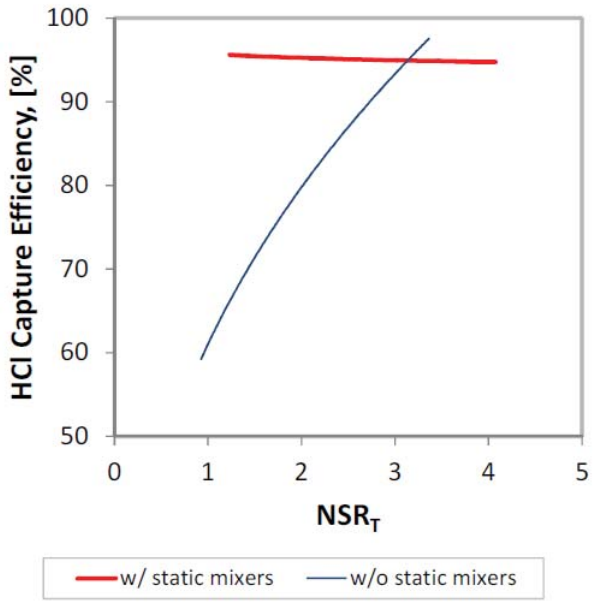

Figure 22: HCl Capture vs. NSR Test Data for Full-scale Sorbent Injection System.

References

1. Goots, T. R., DePero, M. J., and Nolan, P. S. (1992). LIMB Demonstration Project Extension and Coolside Demonstration – Final Report (DOE Report No. DOE/PC/79798-T27). Babcock & Wilcox Company. Retrieved from http://www.osti.gov/scitech/servlets/purl/6935176
2. U.S. Department of Energy. (2000). LIMB Demonstration Project Extension and Coolside Demonstration: A DOE Assessment (DOE Report No. DOE/NETL-2000/1123). Retrieved from http://www.netl.doe.gov/technologies/coalpower/cctc/resources/pdfs/limb/netl1123.pdf
3. Madsen, Jens I., Starns, Travis, Rogers, William A., and O'Brien, Thomas J. (2005). The impact of Turbulent Mixing on Sorbent Dispersion in Coal-Derived Flue Gases. International Conference on Air Quality V. October 19-21, 2005. Arlington, VA.
4. Cremer, Marc, Senior, Constance, Chiodo, Andrew, Wang, David, and Valentine, James. (2005). CFD Modeling of Activated Carbon Injection for Mercury Control on Coal-Fired Power Plants. Presented at Electric Power Conference, April 4-7, 2005, Chicago, IL.
5. Chung, Jin Do, Kim, Jang Woo, and Park, Young Moon. (2010). A Study on Vortex Generators to Improve the Mixing Rate in the Dry Sorbent Injection Process of the Flue Gas Desulfurization System. Korean J. Chem. Eng., 27(1), 83-90.
6. Hopkins, M.W. and Muoh, O. F. (2010, June 6-10). Predicting PAC, Hydrated Lime, and Trona Effectiveness in Flue Gas Systems using CFD and Physical Analyses for Optimized Nozzle Design. Paper presented at the 35th International Technical Conference on Coal Utilization & Fuel Systems, Clearwater, Florida.
7. Senior, Constance, Wang, Huafeng, Wilson, Jeff, and Irvin, Nick. (2009, June 16-19). Computational Fluid Dynamic Modeling of SO3 Capture by Sorbents in Coal Flue Gas. Paper presented at 102nd Air and Waste Management Association Annual Conference and Exhibition, Detroit, MI.
8. Blankinship, Steve. (2006). CFD Modeling Could Optimize Sorbent Injection System Efficiency. Power Engineering Magazine, 110(1)
9. Cremer, Marc A., Wang, David H., and Senior, Connie L. (2008). Testing and Model Based Optimization of SO_2 Removal with Trona in Coal Fired Utility Boilers. Presented at 7th Power Plant Air Pollutant Control Mega Symposium, August 25-28, 2008, Baltimore, MD.
10. Starns, Travis, Martin, Cameron, Mooney, J., and Jaekels, J. (2008). Commercial Operating Experience on an Activated Carbon Injection System. Presented at 7th Power Plant Air Pollutant Control Mega Symposium, August 25-28, 2008, Baltimore, MD.
11. Gentry, Matt. (2013, July 8-9). CFD and Physical Modeling of DSI/ACI Distribution. Poster session presented at the Reinhold APC Round Table & Exposition, St. Louis, MO.
12. Balcke Duerr GmBH brochure. Static Mixers for Flow Optimization. Retrieved from http://www.spx.com/en/assets/pdf/static-gas-mixer.pdf
13. Kong, Yougen and Wood, Michael. Combined Treatment of HCl and SO_2: Independent Study Shows Selectivity and Effectiveness of Sodium Dry Sorbent Injection. Retrieved from http://www.solvair.us/en/binaries/20120726-DSI-White-Paper-202196.pdf

For further Information contact
Matthew Quitadamo at mquitadamo@babcockpower.com

Matthew Quitadamo currently serves as Technical Advisor for Environmental Technology at Babcock Power Environmental Inc. (BPEI). In this role, he is responsible for development projects, engineering quality procedures, and managing the development of design standards for environmental technologies. Since joining BPEI in 2002, Matthew has held various positions in the field of air pollution control for industrial and utility power generation markets, including Process Engineer, CFD Engineer, and Product Manager of Wet Flue Gas Desulfuration. Matthew has a Bachelor of Science in Chemical Engineering, a Master of Science in Mechanical Engineering, and a Master of Science in Environmental Engineering from Worcester Polytechnic Institute.

Babcock Power

WPCA Corporate Sponsors

WPCA Chairman
Susan Reinhold, CEO
Reinhold Environmental Ltd.
3850 Bordeaux Drive, Northbrook, IL 60062 USA
Email: sreinhold@reinholdenvironmental.com

WPCA Secretary
Jason Horn, Dir. of Env. Controls
Stock Equipment Company
16490 Chillicothe Rd, Chagrin Falls, OH 44023
Email: jason.horn@stockequipment.com

WPCA Treasurer
Robert Mudry, President
Airflow Sciences Corporation
12190 Hubbard Street, Livonia, MI 48150 USA
Email: rmudry@airflowsciences.com

WPCA Vice President
Nate White, Dir. Business Development
Haldor Topsoe, Inc.
5510 Morris Hunt Dr., Fort Mill, SC 29708 USA
Email: tnw@topsoe.com

David Novogoratz, Business Dev. Mgr.
Babcock & Wilcox
20 S. Van Buren Ave., Barberton, OH 44203 USA
Email: dmnovogoratz@babcock.com

Clayton Erickson, Manager, Process Eng.
Babcock Power Inc.
5 Neponset Street, Worcester, MA 01606 USA
cerickson@babcockpower.com

Allen Kephart, President
CleanAir Engineering
110 Technology Dr., Pittsburgh, PA 15275
Email: akephart@cleanair.com

Mark Ehrnschwender, VP Bus. Dev&Engr
Steag Energy Services LLC
304 Linwood Rd, Ste.102, Kings Mountain, NC 28086 USA
Email: mark.ehrnschwender@steag.us

Tim Stark, Director
CLARCOR Industril Air
11501 Outlook St., Ste. 100,
Overland Park, KS 66211 USA
Email: timothy.stark@clarcor.com

Richard Staehle, CEO
KC Cottrell, Inc.
8 Bartles Corner Rd., Ste 204,
Flemington, NJ 08822 USA
Email: rstaehle@kccottrell.us

Michael Hatsfelt, General Manager
Southern Environmental, Inc.
6690 West Nine Mile Rd., Pensacola, FL 32526
Email: mhatsfelt@sei-group.com

Gordon Maller, Bus. Development Mgr.
URS Corporation
9400 Amberglen Blvd., Austin, TX 78729 USA
Email: gordon.maller@urs.com

Tom Lugar, VP Product Development
MET
200 North 7th St., Lebanon, PA 17046 USA
Email: tlugar@met.net

Michael Atwell, Market Dev. Mgr.
SOLVAir Sol. Solvay Chemicals
3333 Richmond, Houston, TX 77098 USA
Email: michael.atwell@solvay.com

Jamie Fessenden, Bus. Mgr. Emission
Control Tech \ Cabot Norit Americas
3200 University Ave., Marshall, TX 75670 USA
Email: jfessenden@cabotcorp.com

Curt Biehn, Mgr., Mkt & Tech Services
Mississippi Lime
3870 S. Lindbergh Blvd., St. Louis, MO 63127
Email: crbiehn@mississippilime.com

Paul Ford, President
Redkoh Industries
300 Valley Road, Hillsborough, NJ 08844 USA
Email: paul.ford@redkoh.com

Sharon Sjostrom, Chief Technical Officer
ADA-ES
9135 S. Ridgeline Blvd., Ste 200,
Highlands Ranch, CO 80129 USA
sharons@adaes.com

WPCA Officers

WPCA President
Joseph Hantz, Manager Environmental Services, Entergy

WPCA Vice President
Melissa Allen, Environmental System Engineering Manager, TVA

WPCA Advisors

- **Greg Betenson,**
  Principal Engineer, PacifiCorp
- **Melanie McCoy,**
  Superintendent Sebewaing Light & Power
- **Ebrahim Patel,**
  Senior Consultant - APC, ESKOM-GTD
- **Bruce Salisbury,**
  Engineering Supervisor, Arizona Public Service
- **Scott Williams,**
  Principal Engineer, Duke Energy
- **Grant Hilbers,**
  Supervisor - Engineering, DTE Energy